AIAA JOURNAL
Vol. 36, No. 7, July 1998

Passive Control of Supersonic Rectangular Jets via Nozzle Trailing-Edge Modifications

M. Samimy,* J.-H. Kim,† P. S. Clancy,‡ and S. Martens§
The Ohio State University, Columbus, Ohio 43210

A research program was carried out to explore the effects of nozzle trailing-edge modifications on the flow structure, jet mixing with the ambient air, and jet noise of a rectangular supersonic jet. Nozzles with one modified trailing edge were used with the intention of enhancing mixing and reducing noise. The modifications were simple cutouts in the plane of the nozzle wall and acted to induce large-scale streamwise vortices. A rectangular jet, with a design Mach number of 2 and with various trailing edges, was examined using optical diagnostics and noise measurements in flow regimes ranging from moderately overexpanded $M_j = 1.5$ to moderately underexpanded $M_j = 2.5$. The results indicated that in nonideally expanded flow regimes, one could generate pairs of streamwise vortices of various strength and sign and that the mixing could be significantly enhanced. The results also indicated that the modifications could eliminate or at least substantially reduce screech noise and could significantly decrease the overall far-field sound pressure level in the nonideally expanded flow regimes. In the ideally expanded flow regime, the trailing-edge modifications did not seem to induce streamwise vortices and, thus, did not have a substantial effect on the jet mixing or noise.

Introduction

LARGE-SCALE ring-type rollers in axisymmetric free mixing layers and spanwise rollers in two-dimensional free mixing layers are known to become much less organized and more three dimensional as the compressibility level is increased.[1–3] In highly compressible free shear flows, this leads to reduced entrainment and mixing[4] and also reduced Reynolds stresses.[5–7] Therefore, it is difficult to use spanwise or ring-type large-scale structures to control mixing processes in these flows. In contrast, longitudinal or streamwise vortices seem to be unaffected or much less affected by compressibility.[8,9] In some flows, such as highly underexpanded jets, streamwise vortices may be generated due to Taylor–Goertler-type instabilities without any external device or force.[10–12] Streamwise vortices could also be generated by simple devices, such as tabs, not only in underexpanded jets but also in subsonic and in ideally expanded supersonic jets[8,9,13] and even in very-low-Reynolds-number incompressible jets.[14] At very low Reynolds numbers, streamwise vortices are also generated by secondary instabilities.[15] The primary focus of the present work was to induce large-scale streamwise vortices using nozzle trailing-edge modifications in supersonic jets issuing from rectangular nozzles. The ultimate goal was to obtain mixing enhancement and noise reduction with a minimum loss of thrust force. The trailing-edge modifications explored in this research were all in the plane of the nozzle wall and thus parallel to the flow. Therefore, it was anticipated that the thrust loss due to these trailing-edge modifications would be much lower in comparison with that of other devices, such as tabs. The most recent results indicate that these cutouts have negligible effect on the thrust.[16]

Flows from modified axisymmetric nozzles have been studied in supersonic jets,[17–20] in subsonic jets,[21] and from modified rectangular nozzles in supersonic jets.[22,23] However, all of these researchers concentrated on noise and pressure measurements, except Longmire et al.,[21] who investigated subsonic jets. Detailed flow visualizations and flow measurements were needed to complement the noise and pressure results to further understand the effects of nozzle trailing-edge modifications on the flow structure and mixing processes. One of the goals of the present work was to acquire such flow visualizations and measurements.

The work herein was focused on rectangular nozzles because they have superior mixing and noise characteristics relative to axisymmetric nozzles.[24–32] For the work presented, we selected a half-nozzle geometry with a splitter plate on one side and a nozzle block on the other side. The trailing-edge modifications were made only on the splitter plate side (Fig. 1a). The location of the splitter plate would have been the centerplane of the nozzle had this been a full nozzle. There were two reasons behind this design. First, the design ensured that the flow reached the nozzle design Mach number before approaching the trailing-edge modifications. The design Mach number for the results presented was 2. In the research facility, the flow reached Mach 2 at the nozzle exit on the nozzle side and over 4.4 cm upstream of the nozzle exit on the splitter plate side, along the last characteristic or Mach line. The angle of this line for Mach 2 flow was 30 deg with respect to the flow direction. The nozzle exit was 2.54 cm high and 7.52 cm wide. All of the modifications on the splitter plate terminated 3.8 cm upstream of the nozzle exit and thus 0.6 cm downstream of the establishment of Mach 2 flow. Second, the trailing-edge modifications in only one side allowed us to focus on the induced flow structures due to these modifications alone and to investigate them in detail. The nozzle trailing-edge modifications were simple cutouts in the splitter plate. As shown in Fig. 1, various cutouts were used. The reasons behind the selection of these cutouts will be elaborated on. Note that rectangular nozzles have been used in some recent advanced aircraft. The nozzles in these aircraft have trailing edges formed from trailing-edge elements shown in Fig. 1. However, there is no work in the literature detailing the flowfields of such nozzles.

Experimental Facility and Techniques

The experiments were conducted at the Aeronautical and Astronautical Research Laboratory at The Ohio State University. The air, which was supplied by two four-stage compressors, was filtered, dried, and stored in two cylindrical tanks with a total capacity of 42.5 m^3 at 16.5-MPa pressure. The air was then throttled down to the required stagnation pressure using control valves. The air entered the 19-cm-diam and 120-cm-long stagnation chamber axially and then passed through two sets of perforated plates before entering the nozzle. The rectangular nozzle, with an aspect ratio of 3 (2.54 cm

Received Sept. 22, 1997; revision received March 9, 1998; accepted for publication March 9, 1998.

*Professor and Associate Chairman, Department of Mechanical Engineering. Associate Fellow AIAA.

†Graduate Student, Department of Mechanical Engineering. Member AIAA.

‡Graduate Student, Department of Mechanical Engineering; currently Senior Member of Technical Staff, TRW Space and Electronics Group, Redondo Beach, CA 90278. Member AIAA.

§Postdoctoral Fellow, Department of Mechanical Engineering; currently Aeroacoustic Engineer, General Electric Aircraft Engines, Cincinnati, OH 45215. Member AIAA.

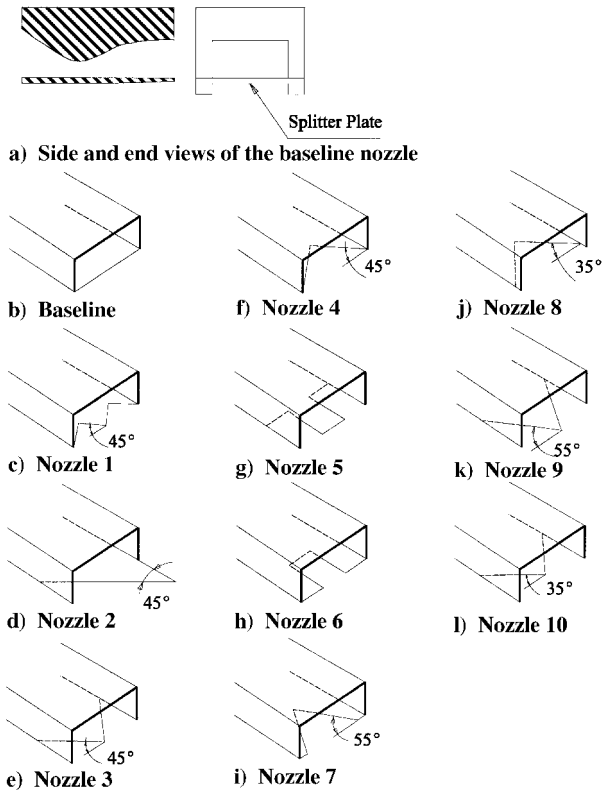

Fig. 1 Schematic of the nozzle trailing-edge configurations.

high and 7.52 cm wide), was attached to the stagnation chamber using a specifically designed faceplate, which provided a matching profile for the nozzle inlet.

Schematics of the baseline nozzle and the 10 nozzles with the modified trailing edges that were used in these experiments are shown in Figs. 1b–1l. As was discussed earlier, the baseline nozzle was a half-nozzle with a splitter plate of 1-mm thickness on one side (Fig. 1a) and the supersonic nozzle block, 44-mm thickness at the exit plane, on the opposite side. The thickness for the other two sides, at the nozzle exit plane, was 19 mm. The rationale behind this design was discussed earlier. It is known that the nozzle lip thickness affects the screech noise because the upstream traveling noise, generated by the unsteady interaction of large structures with the quasistationary shock train in nonideally expanded flow regimes, is scattered by the nozzle lip, and this scattered noise then forces the shear layer of the jet.[33] For the work presented here, the overall effect of the nozzle lip thickness was investigated by replacing the splitter plate of the baseline nozzle with a thick lip plate in some experiments. Each nozzle was operated at five nozzle pressure ratios, corresponding to fully expanded jet Mach numbers of 1.5, 1.75, 2.0 (design Mach number), 2.2, and 2.5. The splitter plate modifications were combinations of simple serrations on the splitter plate. The angle of the serrations with respect to the spanwise direction ranged from 35 to 90 deg.

Cross-sectional and streamwise images of the jet were acquired using the laser sheet illumination technique. The scattering particles were condensed water particles with diameters on the order of 50 nm, which were formed when the moist and warm ambient air was entrained into and mixed with the dry and cold jet air. A beam from the second harmonic ($\lambda = 532$ nm) of a frequency-doubled Nd:YAG pulsed laser was used to form a light sheet. The pulse width of the laser was 9 ns, so that the flow was effectively frozen while an instantaneous image was acquired. For each case, 50 instantaneous images were collected by an intensified charge-coupled device (ICCD) camera and were stored on the hard disk of a 486 personal computer. Average images were calculated from these 50 instantaneous images.

Near- and far-field noise was measured by two B&K Model 4135, 6.35-mm-diam condenser microphones. The microphones were omnidirectional within 3, 6, and 12 dB up to 12.5, 20, and 31.5 kHz, respectively. However, in the noise measurements reported herein, the directivity was within 1 and 2.5 dB up to 20 and 31.5 kHz, respectively, because the microphone axis angle relative to the jet noise sources was less than 40 deg. Each microphone was attached to a B&K Model 2633A preamplifier. The signals from both microphones were amplified by a B&K Model 5935 dual-microphone amplifier. The acoustic signals were acquired by an A/D board at a sampling rate of 100 kHz per channel. The acoustic data were saved on the hard disk of a 486 personal computer; 100 blocks of 4096 samples were acquired with a corresponding total sampling time of 4.096 s. By using a B&K-type 4231 sound level calibrator, which is an electronically driven constant-sound-level generator at 1 kHz, each microphone was calibrated after the acquisition of each data set. For the far-field noise measurements, both microphones were placed 30 nozzle equivalent diameters, $D_{eq} = (4A_e/\pi)^{1/2} = 4.96$ cm, away from the jet centerline on the jet exit plane: one on the major axis and the other on the minor axis of the nozzle. To determine the changes in the screech mode due to the modification of the nozzle trailing edge, limited near-field noise measurements were also performed. For acoustic measurements, the face of the stagnation chamber and all of the nearby surfaces were covered with acoustic foam to reduce acoustic reflections. Note that the jet facility was not located within an anechoic chamber. Therefore, the acoustic measurements reported herein are intended only for comparison of the effects of different trailing-edge modifications on the overall acoustic field.

Experimental Results

In the planning and design phases of the experimental work, it was conjectured that the serrations or cutouts in the splitter plate would induce longitudinal (or streamwise) vortices in the nonideally expanded flow regimes, and in a given flow condition, the sign of vortices for nozzles 3, 5, 9, and 10 (group A) would be opposite to those for nozzles 4, 6, 7, and 8 (group B). In addition, it was postulated that the cutouts would trigger and/or enhance spanwise oblique structures believed to exist in the highly compressible mixing layers of the jet.[1–3,34] Both issues are discussed subsequently. First, the results on the generation of streamwise vortices will be discussed. Then, the effects of cutouts on the oblique spanwise structures, the overall entrainment and mixing, and the jet noise will be addressed.

Streamwise Vortices

In axisymmetric jets with vortex-generating tabs located at the exit of the nozzle, Zaman et al.[9] identified two sources of streamwise vorticity. Source 1, which was the dominant of the two, was the spanwise pressure gradient in front of the tab. Source 2 was the shedding of vorticity from the sides of the tab. Only in some tab configurations did the streamwise vorticity from both sources have the same sign and seem to reinforce each other. At very low Reynolds numbers in incompressible flows, Reeder and Samimy[14] identified a third vorticity source, which was the wrapping of the incoming boundary layer to generate a pair of horseshoe vortices. In the trailing-edge configurations tested herein, a simple experiment was conducted to examine the presence of source 1. In the experiment, seven pressure taps aligned in the spanwise direction immediately upstream of the cutouts in nozzles 3 and 4 did not show an appreciable spanwise pressure gradient. Thus, the presence of source 1 was ruled out. Recall that in the case of Zaman et al.[9] the tabs were protruding into the flow. Thus, one would expect a spanwise pressure gradient in front of the tabs. In the present experiments, the cutouts were in the plane of the nozzle, rather than protruding into the flow. Therefore, one would not expect a spanwise pressure gradient. Therefore, one would anticipate only source 2 to be present in both the ideally expanded and nonideally expanded flow regimes. The shed vorticity would then go through stretching and tilting, as will be discussed.

As shown schematically in Fig. 2, sheets of vorticity are continuously shed from the sides of the cutouts. This is source 2, as was discussed. If one takes a vortex filament from this vortex sheet, it is initially aligned with the side of the cutout (and possesses both Ω_x and Ω_z components in this specific configuration). However, as it convects downstream, the Ω_z component is reoriented by the velocity gradient $\partial U/\partial z$. Bradshaw[35] called this mechanism of mean

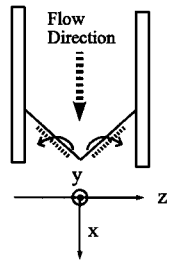

Fig. 2 Schematic of vortex shedding from the trailing edge.

vorticity generation *skew-induced generation*. The shed vorticity shown in Fig. 2 could originate from two sources. Source 2a is the vorticity in the boundary layer in a typical subsonic jet or in the ideally expanded supersonic jet. In the underexpanded or overexpanded flow regimes, there would be a significant pressure gradient aligned with the trailing-edge cutout.[36] This would generate additional vorticity, which is source 2b. Obviously, both sources 2a and 2b would exist in the nonideally expanded flow regimes.

Equation (1) is the transport equation for the mean vorticity in compressible flows.[37] The streamwise component of this equation indicates the inviscid nature of this streamwise vorticity generation process and how the velocity gradient in the shear layer converts Ω_z into Ω_x:

$$\frac{\mathrm{D}(\boldsymbol{\Omega}/\rho)}{\mathrm{D}t} = \frac{\boldsymbol{\Omega}}{\rho}\cdot\nabla\boldsymbol{V} - \frac{1}{\rho}\nabla\left(\frac{1}{\rho}\right)x\nabla P + \text{viscous term} \qquad (1)$$

$$\frac{\mathrm{D}(\Omega_x/\rho)}{\mathrm{D}t} = \frac{\Omega_x}{\rho}\frac{\partial U}{\partial x} + \frac{\Omega_y}{\rho}\frac{\partial U}{\partial y} + \frac{\Omega_z}{\rho}\frac{\partial U}{\partial z}$$

$$+ \text{baroclinic term} + \text{viscous term} \qquad (2)$$

The baroclinic term is a compressible flow phenomenon. Earlier work showed that the overall effects of tabs on the jet cross section were similar in compressible and incompressible jets.[8,9] Thus, the baroclinic term is assumed to be smaller in comparison with the vortex stretching term (first term on the right-hand side) and with the vortex tilting and reorientation term (third term) in Eq. (2). As the flow exits the nozzle in the underexpanded flow regime, there is a flow acceleration in the streamwise direction with a significant density drop. Conversely, there is a flow deceleration in the streamwise direction in the overexpanded flow regime with a significant density increase. In a simple two-dimensional expansion or compression, one could show that the effect of density would outweigh the effects of expansion in the vortex stretching term.[16] However, it is very difficult to assess this term in more complex three-dimensional cases of interest herein. Therefore, we will assume that the effects of the vortex stretching term are also negligible in comparison with those of the vortex reorientation term.

With these assumptions, the generation of streamwise vorticity due to the trailing-edge modifications can be explained using Eq. (1). Good agreement between the trends in the experimental results presented later and those of the predictions based on Eq. (1) lends credibility to these assumptions. Looking at the cutouts shown in Fig. 1, it becomes obvious that, in nozzles 5 and 6 with 90-deg cutouts, there is no need for the reorientation of the shed vorticity filament, as it is already aligned with the streamwise direction. For the other nozzles with angles ranging from 35 to 55 deg, the vorticity filament must be reoriented by the velocity gradients in the shear layer, as indicated in Eq. (1).

To increase the entrainment and mixing via streamwise vortices, each pair of vortices must be sufficiently large and strong, and the vortices in each pair must be placed reasonably far apart from each other (especially when they rotate toward each other) and from other streamwise vortices in the flow. Vortices placed near each other would interact in a destructive manner when they rotate toward each other, earlier in their development stage, and this interaction would limit their growth and, thus, their entrainment potential. For given nozzle operating conditions, the angle and the depth of the cutouts in Fig. 1 are the geometrical parameters that would affect the characteristics of streamwise vortices generated by these cutouts, i.e., the size, the strength, and the distance between the vortices in the pair. For example, both nozzles 1 and 4 have 45-deg cutout angles. However, the depth of the cutouts for nozzle 4 was twice that of nozzle 1. Thus, streamwise vortices generated in nozzle 1 would be smaller scale and closer to each other in comparison with those of nozzle 4. Figure 3 shows the jet cross sections for a slightly underexpanded flow ($M_j = 2.2$) for these two nozzles at 1 and 5 nozzle exit equivalent diameters D_{eq} downstream of the nozzle exit. The images, which are the average of 50 instantaneous images, indicate the average mixing region, where the moist ambient air has been mixed with the cold and dry jet air to generate condensed water particles that scatter the laser light. These particles were very small, with a diameter on the order 50 nm, and were expected to follow the flow.[38]

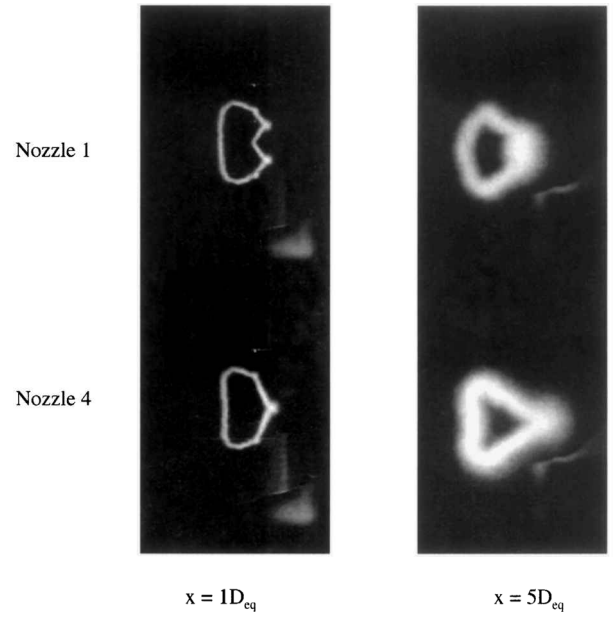

Fig. 3 Average cross-sectional images at two downstream locations for nozzles 1 and 4.

For nozzle 1, as shown in Fig. 3, initially there are two pairs of streamwise vortices. Note that the flow-visualization technique used herein cannot directly measure streamwise vortices. However, the existence of streamwise vortices can be inferred from their effects on the jet cross section. We have successfully used this type of inference in the past. In a recent work, we made some streamwise vorticity measurements in a supersonic jet with a single tab.[39] The results were consistent with the inference that was used in the past.[8,9,14] The vortices in each pair are smaller and closer to each other but have the same strength as the pair of vortices in nozzle 4. Each pair is pulling and stretching the jet cross section (ejecting the jet air into the ambient) and forming a V shape. Farther downstream, the two pairs in nozzle 1 interact, merge by $5D_{eq}$, and become less effective in the large-scale mixing of the jet air with the ambient air. However, the pair of vortices in nozzle 4 continues to grow and mix the jet and ambient air at $5D_{eq}$. Therefore, the impact of streamwise vortices on the overall mixing, and on the acoustic field, should be much greater in nozzle 4 in comparison with nozzle 1. Based on these results, it was decided to fix the depth of the cutouts at 3.8 cm and to change the strength and the distance between a pair of streamwise vortices by using the angles of the cutouts. The mixing performance of nozzle 2 was comparable to those of nozzles 3 and 4 up to several jet diameters but dropped off farther downstream.[40] The variables associated with this nozzle were not easy to fit into a simple test matrix. Therefore, the discussion will focus on the baseline nozzle and nozzles 3–10. Nozzles 3, 5, 9, and 10 (group A) and nozzles 4, 6, 7, and 8 (group B) were chosen to generate vortices of opposite sign to evaluate the effects of entrainment vs ejection in a given flow regime. Various cutout angles were used because the cutout angle determines the strength of the streamwise component of shed vortices for a given flow condition, as already discussed. It was thought that the various spanwise-oblique angles from 35 to 55 deg would also help to shed some light on the excitation of oblique spanwise structures, as will be further discussed later.

Flow-Visualization Results

Figures 4 and 5 show instantaneous and average jet cross-sectional images for the baseline nozzle and nozzles in group A [3(45 deg), 5(90 deg), 9(55 deg), and 10(35 deg)]. These instantaneous images are typical: All contain structures with scales as large as and often even larger than the average thickness of the mixing layer and extend far beyond the mixing region. The average images are ensemble averages over 50 instantaneous images. The overall jet cross-section deformations appear to be quasi-spatially stationary for this location. The differences in the jet cross sections at the ideally expanded flow regime, $M_j = 2.0$, for various nozzles are minor. This is consistent with the hypothesis on the generation of streamwise vortices, as discussed earlier. It also indicates that these cutouts do not affect, in a measurable way, the spanwise structures. This issue will be further discussed later.

It is known that a pair of streamwise vortices is generated at each corner of a rectangular nozzle.[32] Evidence of corner vortices in the baseline case is presented in Figs. 4 and 5 for $M_j = 2.5$ only. By $x/D_{eq} = 2$, it is not clear if two pairs from adjacent corners have merged to form a single pair that pulls and stretches the jet along the major axis. The effects of these streamwise vortices would be similar on the jet cross section with or without the pairing.

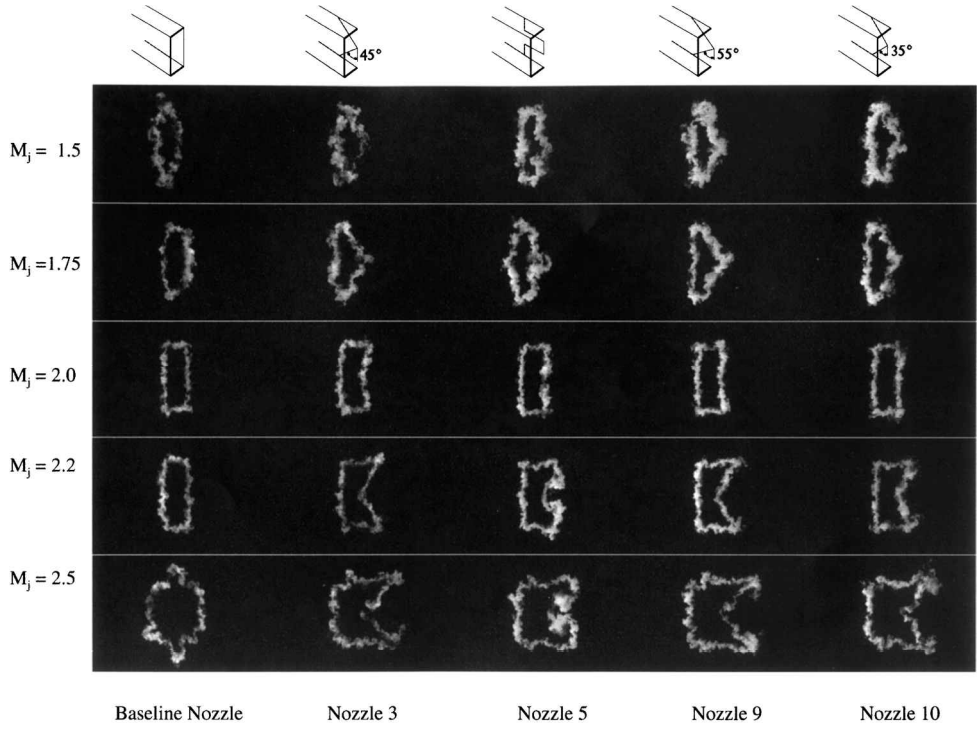

Fig. 4 Instantaneous cross-sectional images for the baseline and group A nozzles at $x = 2D_{eq}$.

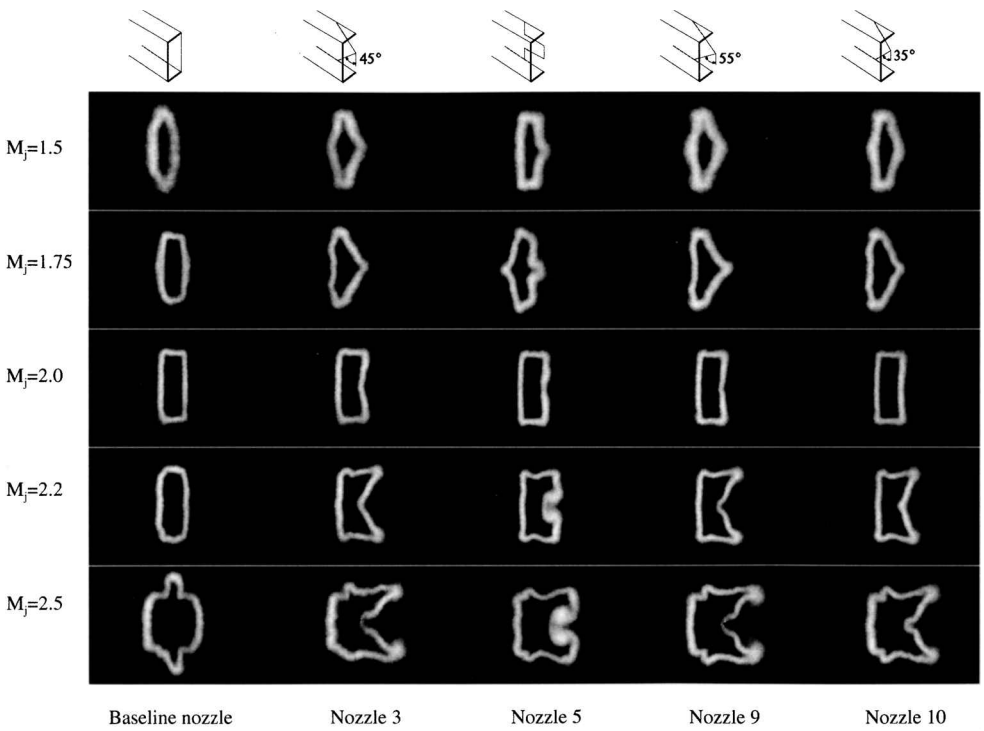

Fig. 5 Average cross-sectional images for the baseline and group A nozzles at $x = 2D_{eq}$.

The streamwise vortices due to the cutouts in the overexpanded flow regime are weaker, most probably due to the lower surface pressure gradients normal to the cutouts in comparison with those in the underexpanded flow regime.[36] The vortices in the pair are also closer to each other as the jet cross section is compressed, in comparison with those generated in the underexpanded cases as the jet cross section is expanded. Both effects render the vortices in the overexpanded case to be less effective in deforming the jet cross section. For the modified nozzles, the direction of the vortices and, thus, the direction of the deformations change from the overexpanded cases to the underexpanded cases. This is intuitive because the direction of the surface pressure gradient changes from the overexpanded cases to the underexpanded cases due to the boundary conditions at the nozzle exit.

As was discussed earlier, for each one of the group A nozzles in the underexpanded flow regimes shown in Figs. 4 and 5, there is a pair of streamwise vortices, both rotating toward the minor axis of the jet. These vortices entrain ambient air into the jet. Note that, due to the nature of the technique, the visualizations detect only the portion of the mixing layer between the jet and the ambient air that has condensed water particles from the mixing of the moist and warm ambient air with the cold and dry jet air. Therefore, the technique could not directly visualize streamwise vortices in all cases, but their presence could easily be inferred from some of the images. The images such as those for nozzle 5 at $M_j = 2.2$ and 2.5, for example, display convincing evidence for the presence of streamwise vortices. In the overexpanded case with $M_j = 1.75$ for each nozzle, there is a pair of vortices with signs opposite to those of the underexpanded cases. These vortices eject the jet air into the ambient and stretch the jet cross section along the jet minor axis. However, the picture is not as clear for the $M_j = 1.5$ cases, as the strong pressure gradient at the nozzle exit compresses the jet cross section and constrains the growth and development of streamwise vortices.

Figure 6 shows the average jet cross-sectional images for the baseline nozzle and group B nozzles [4(45 deg), 6(90 deg), 7(55 deg), and 8(35 deg)]. The main difference between these nozzles and the group A nozzles is that the cutouts were inverted. In the interest of space, the instantaneous images for these nozzles are not presented. The comparison between the average and instantaneous images for these nozzles is similar to that shown in Figs. 4 and 5 (Ref. 41). Comparing the images shown in Fig. 6 with those in Fig. 4, one notices, as expected, the change in the direction of rotation of the dominant streamwise vortex pairs and the jet cross-section deformation for the inverted cutouts. For example, in underexpanded flow regimes for nozzle 5, the vortices are rotating toward the jet minor axis and, thus, entraining the ambient air into the jet; in nozzle 6 they are rotating away from the minor axis and, thus, ejecting the jet air into the ambient. Another difference is that, even at the moderately overexpanded flow condition of $M_j = 1.5$, the streamwise vortices for nozzle 6 are quite strong in comparison with those of nozzle 5.

As was discussed earlier, the depth of the cutouts was fixed for nozzles 3–10. Therefore, for nozzles 3, 4, and 7–10, the angle of the cutouts controls the strength of the vortices and the distance between two adjacent vortices. For nozzles 5 and 6, the angle of the cutouts still controls the strength of the vortices, but the width of the cutouts (or tabs) controls the distance between two adjacent vortices. In the present experiments, the cutout (or tab) width for nozzles 5 and 6 was 2.54 cm ($\frac{1}{3}$ the span of the nozzle). In the group A nozzles, nozzle 5 with 90-deg cutout, and in the group B nozzles, nozzle 6 with 90-deg cutout generate the strongest vortex pair. The results shown in Figs. 4–6 confirm the assertion from Eq. (1) that nozzles 5 and 6, due to the alignment of the cutouts with the vorticity source, would generate much stronger streamwise vorticity in comparison with all other nozzles with angles ranging from 35 to 55 deg.

For any angles other than 90 deg, the angle of the cutouts determines not only the strength of the streamwise vortices but also the proximity of the two vortices in a pair and, thus, the entrainment (or the ejection) rate. For example, the two dominant vortices in nozzle 7 with a 55-deg cutout are much closer to each other than those in nozzle 8 with a 35-deg cutout. This factor, as well as the vortex strength, would affect downstream development and mixing of the jet. For a pair of vortices with circulation Γ and distance r_0, the entrainment (or ejection) rate is proportional to Γ/r_0 (Ref. 32). Therefore, for a given Γ (for example, in nozzles 5 and 6 for a fixed M_j), a smaller r_0 would have more impact in the near field and a larger r_0 more impact in the far-field flow structure and mixing.

Figures 7 and 8 show instantaneous and average images for the baseline nozzle and nozzles 3–6 at eight equivalent jet diameters downstream. There are very large structures in the instantaneous images, some of which extend far beyond the mixing region. For many of the instantaneous images, one could not identify the type of the nozzle. By this location in the jet, there is not much qualitative difference between the average jet cross-sectional image for nozzles

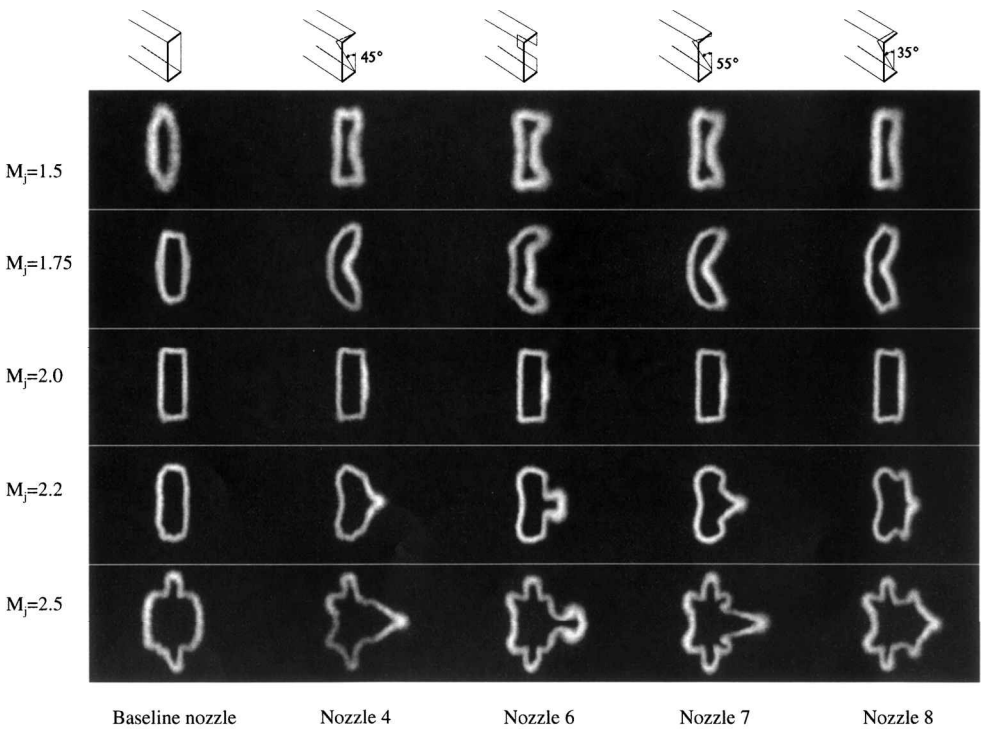

Fig. 6 Average cross-sectional images for the baseline and group B nozzles at $x = 2D_{eq}$.

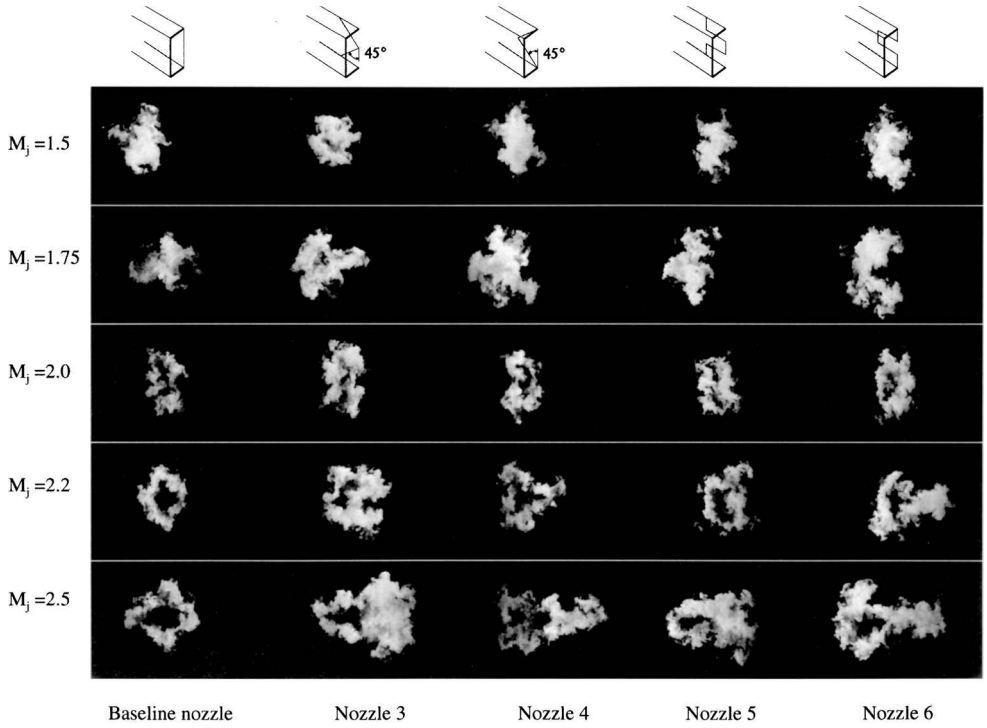

Fig. 7 Instantaneous cross-sectional images at $x = 8D_{eq}$.

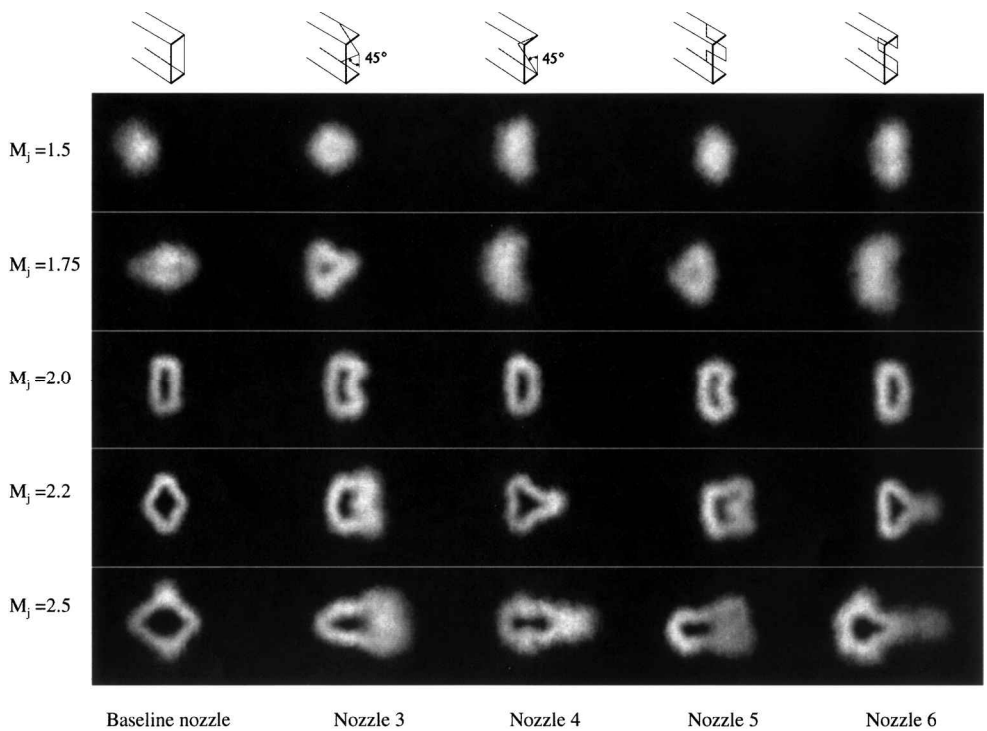

Fig. 8 Average cross-sectional images at $x = 8D_{eq}$.

3 and 5 and 4 and 6. Axis switching has occurred for all of the modified nozzles in the moderately underexpanded $M_j = 2.5$ case. There is strong interaction between two adjacent vortices in nozzles 3 and 5 for this flow condition. The dominant vortices in nozzles 4 and 6 continue stretching the jet along the jet minor axis in the underexpanded flow regimes.

Spanwise Structures

For a Mach 2 jet issuing into ambient air in the present experiments, the convective Mach number in the mixing layer of the jet was approximately 0.85. This corresponds to an angle of 45 deg for the most amplified oblique instabilities according to the theoretical work of Sandham and Reynolds.[34] In choosing the cutout angles in the nozzle trailing-edge modifications, the goal was not only to generate streamwise vortices but perhaps also to trigger and excite the oblique spanwise structures. It is important to note that the phenomenon of gradual switching from two-dimensional instabilities to oblique instabilities in free mixing layers, as the convective Mach number increases beyond approximately 0.6, has been widely reported in the literature based on theoretical and computational work.[34,42–44] However, the experimental results confirm the transition from more organized two-dimensional structures to three-dimensional disorganized structures rather than to organized oblique structures.[1–3]

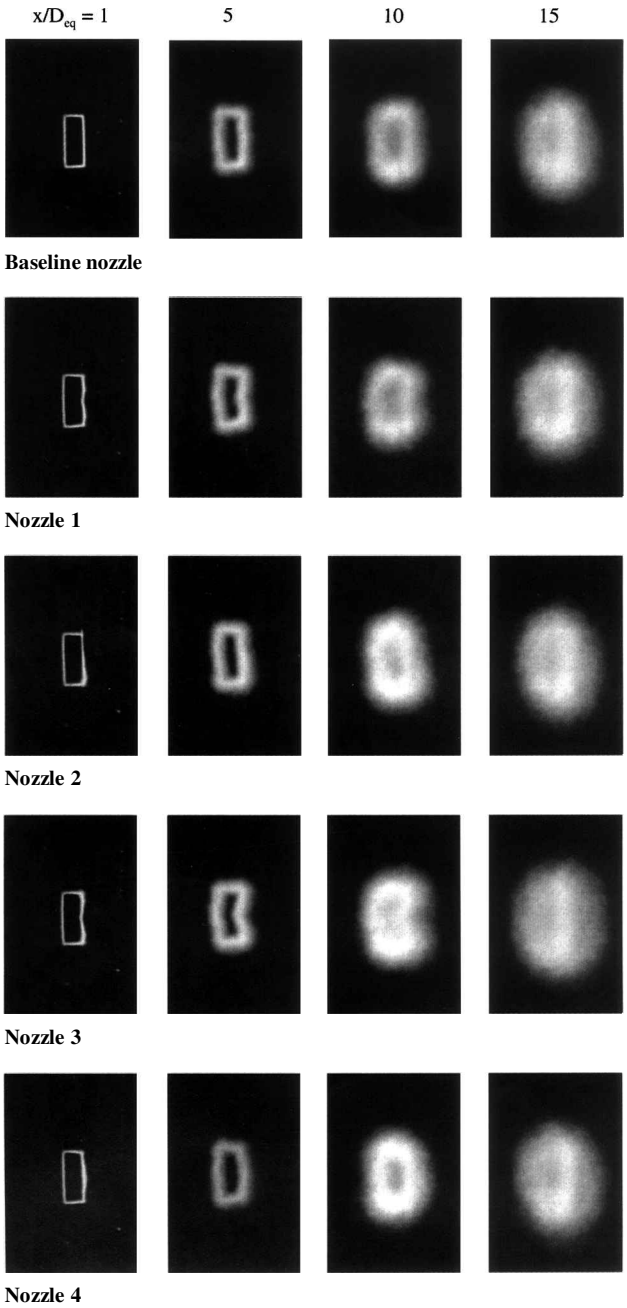

Fig. 9 Average cross-sectional images for the perfectly expanded flow at x/D_{eq} = 1, 5, 10, and 15.

In preliminary experiments, only 45-deg angle serrations were used (nozzles 1–4). Figure 9 shows the average cross-sectional images for the baseline nozzle and nozzles 1–4 in the ideally expanded flow regime in four streamwise locations. Recall that any change in the mixing layer or the jet cross section in the ideally expanded case would come from either excitation of oblique structures or streamwise vorticity generated by the cutouts or a combination of both. As was discussed earlier, the streamwise vorticity for the ideally expanded flow regime is much weaker than the nonideally expanded flow regimes. At $x/D_{eq} = 1$, the baseline nozzle shows an almost perfectly rectangular mixing region. This continues until $x/D_{eq} = 10$. The other nozzles show some variations in their mixing region on the side corresponding to the different trailing-edge modifications. The thicker portions of the shear layer correspond to the locations of the cutouts in the trailing edge. These variations are not thought to be due to the excitation of oblique instability modes but simply due to the earlier formation of the shear layer in the cutout regions, allowing more distance for the shear layers to grow by a given x location, in comparison with the mixing layer of the baseline case. At $x/D_{eq} = 15$ all of the nozzles show elliptical jet cross section with little evidence of the potential core. Again, these images show little difference in the width of the shear layers, although at $x/D_{eq} = 15$ for nozzle 3, the shear layer is slightly thicker than the others. An interesting observation is that there is no sign of axis switching for any of the nozzles up to 15 equivalent diameters from the nozzle exit for the perfectly expanded flow regime.

In the present experiments, we also used 35- and 55-deg cutouts (nozzles 7–10). Qualitatively, the average images in the ideally expanded flow regime for these nozzles in Figs. 5 and 6 do not show any measurable change in the mixing layer or in the jet cross section that one could attribute to the excitation of oblique spanwise structures. Therefore, contrary to our expectation, the cutouts did not seem to excite spanwise oblique structures in the ideally expanded case.

Overall Mixing

To assess the overall mixing performance of the nozzles with various trailing-edge modifications, one must determine the extent of the mixing region between the jet and the ambient air. For the reason discussed next, the calculations must be done on instantaneous images. Then, the average overall mixing must be calculated from the instantaneous mixing. The average images for $M_j = 1.75$ for the baseline nozzle shown in Figs. 5 and 6 indicate a thicker mixing layer in comparison with that of the other nozzles. However, the jet for this case was screeching and flapping.[45] The instantaneous images for this case clearly indicated the effects of this flapping motion, which causes an alternating preferential entrainment and mixing on one side or the other of the mixing layer. Because of this flapping motion, the average jet mixing layer thickness may appear to have increased when in actuality the thickened mixing layer was due to the flapping motion. Therefore, the more accurate calculation of the mixing is to determine the instantaneous mixing first and then to average the instantaneous values to determine the average mixing.

To calculate the average overall mixing area, a threshold intensity level of approximately four times the background level was chosen. Then any pixel in an instantaneous image that had an intensity level higher than this threshold level was counted as a part of the mixing region. First, the instantaneous mixing area was obtained by adding all of the pixels registering an intensity level above the threshold level. Then the average overall mixing area was obtained as an ensemble average of the 50 instantaneous mixing areas. It should be emphasized that this is an approximate measure of the mixing performance of the nozzles and a good tool for comparison purposes. It is by no means a quantitative technique for mixing measurements.

In calculating the mixing areas shown in Fig. 10, we first divided the image for the ideally expanded flow regime along the major axis into two regions; one half was affected and the other half was unaffected by the trailing-edge modifications. Then, we doubled the mixing area in the unaffected half and used it to normalize all of the mixing areas for that nozzle operating in various flow regimes. The reason for this normalization was that the mixing area was visualized based on condensed water particles within the mixing area. These particles were by-products of the mixing of the cold and dry jet air with the warm and moist ambient air. It is believed that the extent of the mixing obtained from the visualization would, to some degree, depend on the ambient temperature and humidity levels. The experiments were conducted in a laboratory environment with no control on these two parameters over a period of several months. Therefore, normalizing the mixing area, as done in Fig. 10, would remove this ambiguity.

Figure 10 shows the overall mixing area for each nozzle at five different flow conditions in the jet near-field region ($2D_{eq}$). As one observes visually from the images, the effects of various cutouts in the ideally expanded flow regime are relatively small in comparison with those in the nonideally expanded flow regimes. In the latter cases, mixing enhancement up to 50% could be seen, and nozzles 5 and 6 outperformed all of the other nozzles in underexpanded and overexpanded flow regimes, respectively. Recall that the vorticity transport equations [Eqs. (1) and (2)] predicted that nozzles 5 and 6 would generate the strongest streamwise vortices, and this was confirmed qualitatively by visualizations shown in Figs. 4–6. Notice that, comparing the performance of nozzles in group A (nozzles 3, 5, 9, and 10) and in group B (nozzles 4, 6, 7, and 8), the former

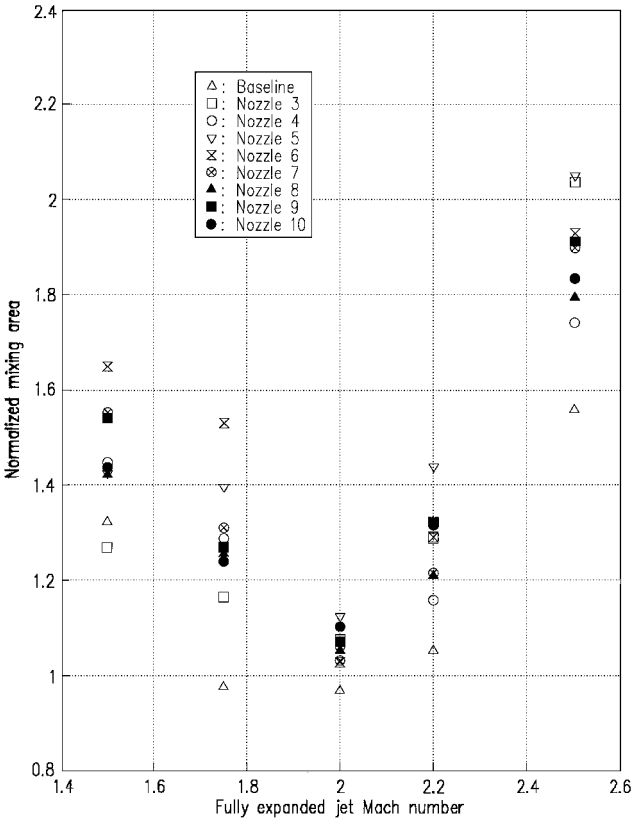

Fig. 10 Variations of mixing area with the fully expanded jet Mach number at $x/D_{eq} = 2$.

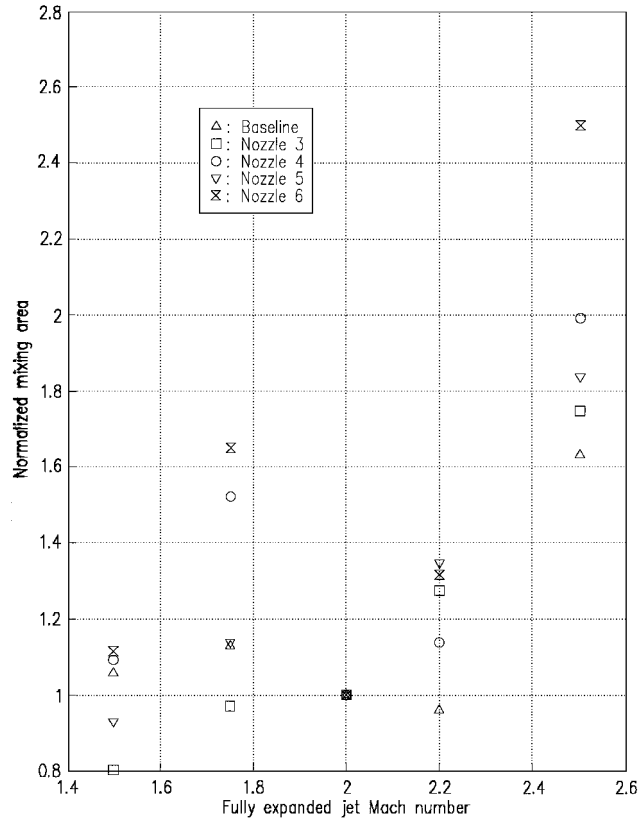

Fig. 11 Variations of mixing area with the fully expanded jet Mach number at $x/D_{eq} = 8$.

has, in general, superior performance in the underexpanded flow regime, whereas the latter has superior performance in the overexpanded flow regime. The streamwise vortices generated by the cutouts in group A nozzles entrain the ambient air into the jet in the underexpanded flow regime, whereas in the group B nozzles, they entrain the ambient air into the jet in the overexpanded flow regime. Therefore, it seems that, in the near-field region, entrainment rather than ejection is more beneficial to mixing. This seems to be true in the jet near field. However, the results for the jet far field, presented next, are somewhat different.

The procedure just outlined could not be used farther downstream, where the cutouts affect the entire cross section of the jet, as seen in Figs. 7 and 8. We noticed the effects of the ambient temperature and humidity after all of the data were taken. For future work, however, the plan is to take a baseline case just prior to or just after each test so each case could be normalized with the baseline case subjected to the same environmental conditions. Because the results presented in Fig. 10 showed that the cutouts have minor effects in the ideally expanded case, for $8D_{eq}$ results (Figs. 7 and 8) it was decided to normalize the mixing region for each nozzle in different flow regimes with the mixing region for the same nozzle in the ideally expanded flow regime. The results for the baseline nozzle and nozzles 3–6 are shown in Fig. 11. This normalization might affect the results by 5–10%, but it should not change the overall trend in a major way. At this jet far-field location, the cutouts still show mixing enhancement of over 50%, and nozzles 6 and 4 outperform nozzles 3 and 5. At this location, nozzle 6 seems to outperform nozzle 5, even in the overexpanded flow regime. Our recent work in two more axial locations confirms the general trends observed herein.[16]

Jet Noise

In this section, the far-field noise results for the baseline nozzle and nozzles 1–4 will be presented and discussed briefly. More detailed treatment of the far-field noise and also the near-field results can be found in Ref. 45.

Two microphones, both located on the exit plane of the jet, $30D_{eq}$ from the jet centerline, one on the minor and the other on the major axis of the nozzle, were used for far-field acoustic measurements. Both microphones showed very similar power spectra. In addition, the overall sound pressure level differences between the two microphones were within the repeatability level of the measurements, which was approximately 0.6 dB. Therefore, only the results from the microphone on the minor axis will be presented and discussed. The standard sound pressure level spectra for all five operating flow conditions for the baseline nozzle and nozzles 3 and 4 were obtained. Screech was observed only in the overexpanded Mach 1.75 case with the first to fifth harmonics of the screech tone being noticeable in the spectrum. In the Mach number 1.5, 2.2, and 2.5 cases, the broadband shock noise was relatively well defined, with no noticeable screech tone. For these cases, either the screech feedback loop was not fully closed or the screech was not sufficiently strong to register at the microphone location, which was 90 deg to the jet axis. It is known that the second harmonic of screech peaks at 90 deg, whereas the first harmonic peaks at an angle of about 150 deg from the jet axis.[18] Replacing the thin-lip (1-mm-thick) baseline nozzle with a thick lip (4.4 cm), the change in the overall sound pressure level was within the repeatability of the measurements. A noticeable difference was that, in the thick-lip case, a relatively weak screech appeared for the slightly underexpanded case of Mach 2.2. As was discussed earlier, the thick lip provides a larger area and, thus, stronger scattering of the upstream traveling shock-associated noise. This would translate into perhaps a more effective forcing of the shear layer of the jet and, thus, the appearance of screech tone.

For the screeching case of Mach 1.75, nozzle 3 eliminated the screech tone, and nozzle 4 substantially reduced its amplitude. Nozzles 1 and 2, however, either did not affect or only slightly affected the screech tone. Figure 12 shows the overall sound pressure level for the baseline nozzle with thin and thick lips and for nozzles 1–4 at all five operating conditions. As can be seen, none of the nozzles affected the overall sound pressure level for the ideally expanded flow regime. As was discussed earlier, this is not surprising because the streamwise vortices are very weak or not existent for this operating regime, and apparently, the cutouts do not seem to affect the spanwise structures. Nozzle 3 was the only one that affected the overall sound pressure level in all off-design conditions in a considerable

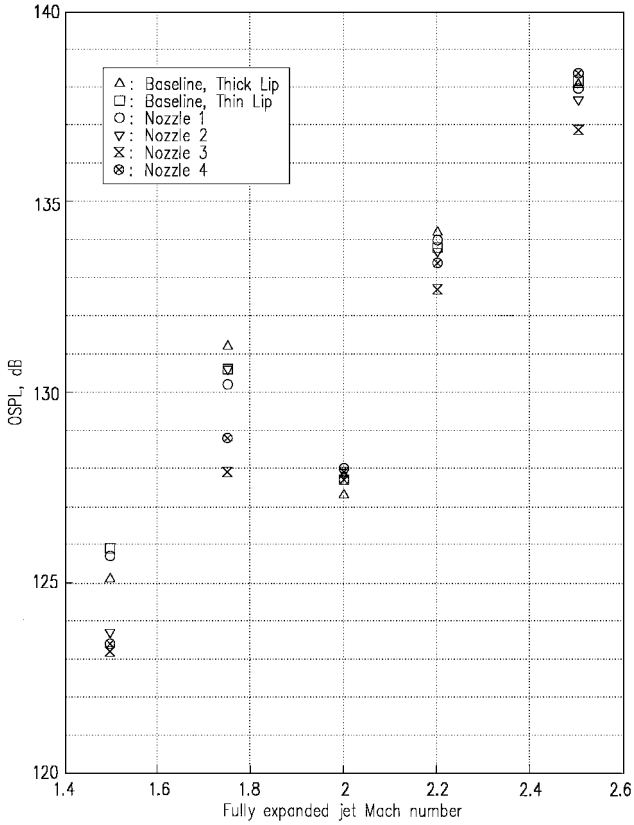

Fig. 12 Far-field noise variations with the jet Mach number.

way: approximately 2.7-dB reduction in the overexpanded cases and 1.2-dB reduction in the underexpanded cases. Nozzle 3 not only effectively eliminated the screech tone but also reduced the broadband shock-associated noise.

The reader should be reminded that in these experiments one side of the nozzle was modified; thus, the effects of the modified geometries on the flowfield could be isolated to understand the physics of the flowfield. However, all four sides of the nozzles could be modified to obtain much better performance. Obviously, this is not a linear process, but one would expect to see much larger effects when all four sides of the nozzle exit are modified judiciously. Further results on the far-field and also near-field noise can be found in Ref. 45.

Conclusions

An extensive research program was carried out to explore the effects of nozzle trailing-edge modifications on the flow structure and mixing performance in rectangular supersonic jets. Several nozzles with one modified trailing edge were used to generate large-scale longitudinal (or streamwise) vortices to enhance mixing and reduce jet noise. The trailing-edge modifications were simple cutouts in the plane of the nozzle wall and acted to induce streamwise vortices. The flow structure, mixing performance, and jet noise of a rectangular nozzle with design Mach number 2 and with various trailing edges were examined using optical diagnostic techniques and acoustic measurements in flow regimes ranging from moderately overexpanded $M_j = 1.5$ to moderately underexpanded $M_j = 2.5$. The results indicated that, in the nonideally expanded flow regimes, one could generate pairs of streamwise vortices of various strength and sign. These vortices would increase entrainment and ejection and also would increase the jet interfacial area, thus increasing the overall mixing and reducing noise, in some cases. The mean streamwise vorticity transport equation was used to describe the generation of these vortices. The sign and the strength of the streamwise vortices generated by the cutouts were consistent with the prediction of this equation. The trailing-edge modifications did not seem to induce streamwise vortices nor to excite spanwise oblique structures in the ideally expanded flow regime and, thus, did not have a considerable effect on mixing or noise for this case.

Acknowledgments

The support of this research by NASA Lewis Research Center through Grant NAG3-1986, K. B. Zaman, Technical Monitor, and by the Air Force Office of Scientific Research through Grant F49620-97-1-0493, M. N. Glauser, Technical Monitor, is greatly appreciated. The authors would like to thank William Erskine for his help in the experimentation and in the editing of the manuscript.

References

[1]Elliott, G. S., Samimy, M., and Arnette, S. A., "Study of Compressible Mixing Layers Using Filtered Rayleigh Scattering Based Visualizations," *AIAA Journal*, Vol. 30, No. 10, 1992, pp. 2567–2569.

[2]Clemens, N. T., and Mungal, M. G., "Two- and Three-Dimensional Effects in the Supersonic Mixing Layer," *AIAA Journal*, Vol. 30, No. 4, 1992, pp. 973–981.

[3]Samimy, M., Reeder, M. F., and Elliott, G. S., "Compressibility Effects on Large Structures in Free Shear Flows," *Physics of Fluids A*, Vol. 4, No. 6, 1992, pp. 1251–1258.

[4]Papamoschou, D., and Roshko, A., "The Compressible Turbulent Shear Layer: An Experimental Study," *Journal of Fluid Mechanics*, Vol. 197, 1988, pp. 453–477.

[5]Samimy, M., and Elliott, G. S., "Effects of Compressibility on the Characteristics of Free Shear Layers," *AIAA Journal*, Vol. 28, No. 3, 1990, pp. 439–445.

[6]Goebel, S. G., and Dutton, C. J., "Experimental Study of Compressible Turbulent Mixing Layers," *AIAA Journal*, Vol. 29, No. 4, 1991, pp. 538–546.

[7]Bonnet, J. P., Debisschop, J. R., and Chambres, O., "Experimental Studies of the Turbulent Structure of Supersonic Mixing Layer," AIAA Paper 93-0217, Jan. 1993.

[8]Samimy, M., Zaman, K. B. M. Q., and Reeder, M. F., "Effect of Tabs on the Flow and Noise Field of an Axisymmetric Jet," *AIAA Journal*, Vol. 31, No. 4, 1993, pp. 609–619.

[9]Zaman, K. B. M. Q., Samimy, M., and Reeder, M. F., "Control of an Axisymmetric Jet Using Vortex Generators," *Physics of Fluids*, Vol. 6, No. 2, 1994, pp. 778–793.

[10]Novopashin, S. A., and Perepelkin, A. L., "Axial Symmetry Loss of a Supersonic Turbulent Jet," *Physics Letters A*, Vol. 135, No. 4, 1989, pp. 290–293.

[11]Krothapalli, A., Buzyna, G., and Lourenco, L., "Streamwise Vortices in an Underexpanded Axisymmetric Jet," *Physics of Fluids A*, Vol. 3, No. 8, 1991, pp. 1848–1851.

[12]Arnette, S. A., Samimy, M., and Elliott, G. S., "On Streamwise Vortices in High Reynolds Number Supersonic Axisymmetric Jets," *Physics of Fluids A*, Vol. 5, No. 1, 1993, pp. 187–202.

[13]Ahuja, K. K., and Brown, W. H., "Shear Flow Control by Mechanical Tabs," AIAA Paper 89-0994, Jan. 1989.

[14]Reeder, M. F., and Samimy, M., "The Evolution of a Jet with Vortex-Generating Tabs: Real-Time Visualization and Quantitative Measurements," *Journal of Fluid Mechanics*, Vol. 311, 1996, pp. 73–118.

[15]Liepmann, D., and Gharib, M., "The Role of Streamwise Vorticity in the Near-Field Entrainment of Round Jets," *Journal of Fluid Mechanics*, Vol. 245, 1992, pp. 643–658.

[16]Kim, J.-H., Samimy, M., and Erskine, W. R., "Mixing Enhancement with Minimal Thrust Loss in a High Speed Rectangular Jet," AIAA Paper 98-0696, Jan. 1998.

[17]Pannu, S. S., and Johannesen, N. H., "The Structure of Jets from Notched Nozzles," *Journal of Fluid Mechanics*, Vol. 74, 1976, pp. 515–528.

[18]Norum, T. D., "Screech Suppression in Supersonic Jets," *AIAA Journal*, Vol. 21, No. 2, 1983, pp. 235–240.

[19]Wlezien, R. W., and Kibens, V., "Influence of Nozzle Asymmetry on Supersonic Jets," *AIAA Journal*, Vol. 26, No. 1, 1988, pp. 27–33.

[20]Krothapalli, A., McDaniel, J., and Baganoff, D., "Effects of Slotting on the Noise of an Axisymmetric Supersonic Jet," *AIAA Journal*, Vol. 28, No. 12, 1990, pp. 2136–2144.

[21]Longmire, E. K., Eaton, J. K., and Elkins, C. J., "Control of Jet Structure by Crown-Shaped Nozzles," *AIAA Journal*, Vol. 30, No. 2, 1992, pp. 505–512.

[22]Rice, E. J., and Raman, G., "Supersonic Jets from Beveled Rectangular Nozzles," *ASME Winter Annual Meeting* (New Orleans, La), American Society of Mechanical Engineers, New York, 1993, pp. 485–490; also ASME Paper 93-WA/NCA-26, Nov.–Dec. 1993.

[23]Raman, G., "Screech Tones from Rectangular Jets with Spanwise Oblique Shock-Cell Structures," AIAA Paper 96-0643, Jan. 1996.

[24]Trentacoste, N., and Sforza, P., "Further Experimental Results for Three-Dimensional Free Jets," *AIAA Journal*, Vol. 5, No. 5, 1967, pp. 885–891.

[25]Krothapalli, A., Baganoff, D., and Karamcheti, K., "On the Mixing of a Rectangular Jet," *Journal of Fluid Mechanics*, Vol. 107, 1981, pp. 201–220.

[26]Tsuchiya, Y., Horikoshi, C., and Sato, T., "On the Spread of Rectangular Jets," *Experiments in Fluids*, Vol. 4, 1986, pp. 197–204.

[27]Gutmark, E., Schadow, K. C., and Wilson, K. J., "Noncircular Jet Dynamics in Supersonic Combustion," *Journal of Propulsion and Power*, Vol. 5, No. 5, 1989, pp. 529–533.

[28]Gutmark, E., Schadow, K. C., and Bicker, C. J., "Near Acoustic Field and Shock Structure of Rectangular Supersonic Jets," *AIAA Journal*, Vol. 28, No. 7, 1990, pp. 1163–1170.

[29]Seiner, J. M., "Fluid Dynamics and Noise Emission Associated with Supersonic Jets," *Studies in Turbulence*, edited by T. B. Gatski, S. Sarkar, and C. G. Speziale, Springer–Verlag, Berlin, 1991.

[30]Raman, G., and Rice, E. J., "Instability Modes Excited by Natural Screech Tones in a Supersonic Rectangular Jet," *Physics of Fluids A*, Vol. 6, No. 12, 1994, pp. 3999–4008.

[31]Grinstein, F. F., "Entrainment and Transition to Turbulence in Subsonic Rectangular Jets," AIAA Paper 95-0861, Jan. 1995.

[32]Zaman, K. B. M. Q., "Axis Switching and Spreading of an Asymmetric Jet: The Role of Coherent Structure Dynamics," *Journal of Fluid Mechanics*, Vol. 316, 1996, pp. 1–27.

[33]Tam, C. K. W., "Supersonic Jet Noise," *Annual Review of Fluid Mechanics*, Vol. 27, 1995, pp. 17–43.

[34]Sandham, N. D., and Reynolds, W. C., "Three-Dimensional Simulations of Large Eddies in the Compressible Mixing Layers," *Journal of Fluid Mechanics*, Vol. 224, 1991, pp. 133–158.

[35]Bradshaw, P., "Turbulent Secondary Flows," *Annual Review of Fluid Mechanics*, Vol. 19, 1987, pp. 53–74.

[36]Kim, J.-H., "An Experimental Study of Mixing Enhancement and Noise Reduction in a Supersonic Rectangular Jet Through Trailing Edge Modifications," Ph.D. Dissertation, Dept. of Mechanical Engineering, The Ohio State Univ., Columbus, OH, 1998.

[37]Morkovin, M. V., "Mach Number Effects on Free and Wall Turbulent Structures in Light of Instability Flow Interactions," *Studies in Turbulence*, edited by T. B. Gatski, S. Sarkar, and C. G. Speziale, Springer–Verlag, Berlin, 1992.

[38]Samimy, M., and Lele, S. K., "Motion of Particles with Inertia in a Compressible Free Shear Layer," *Physics of Fluids A*, Vol. 3, No. 8, 1991, pp. 1915–1923.

[39]Clancy, P. S., and Samimy, M., "Velocity and Vorticity Measurements in Supersonic Jets Modified with a Vortex Generating Tab," Proceedings of 1998 American Society of Mechanical Engineers, Fluid Engineering Div., Summer Meeting, Washington, DC (to be presented).

[40]Martens, S., Samimy, M., and Milam, D. M., "Mixing Enhancement in Supersonic Jets via Trailing Edge Modifications," *Proceedings of 1997 ASME Fluid Engineering Division Summer Meeting*, FED-Vol. 237, Vol. 2, American Society of Mechanical Engineers, New York, 1996, pp. 485–490.

[41]Samimy, M., Kim, J.-H., and Clancy, P., "Mixing Enhancement in Supersonic Jets via Nozzle Trailing Edge Modifications," AIAA Paper 97-1877, June 1997.

[42]Jackson, T. L., and Grosch, C. E., "Inviscid Spatial Stability of a Compressible Mixing Layer," *Journal of Fluid Mechanics*, Vol. 208, 1989, pp. 609–637.

[43]Morris, P. J., Giridharan, M. G., and Viswanathan, K., "Turbulent Mixing in Plane and Axisymmetric Shear Layers," AIAA Paper 90-0708, Jan. 1990.

[44]Gathmann, R. J., Si-Ameur, M., and Mathey, F., "Numerical Simulation of Three Dimensional Natural Transition in the Compressible Confined Shear Layer," *Physics of Fluids A*, Vol. 5, 1993, pp. 2946–2957.

[45]Samimy, M., Kim, J.-H., and Clancy, P., "Supersonic Jet Noise Reduction and Mixing Enhancement Through Nozzle Trailing Edge Modifications," AIAA Paper 97-0146, Jan. 1997.

G. M. Faeth
Editor-in-Chief